# MODELLING ASTEROID TRAJECTORY IN EARTH'S ATMOSPHERE

Renato Henriques Morais[1], Luís Filipe Ferreira Marques[1,2], André Resende Rodrigues da Silva[1] & Rui Melicio[1,3]

[1]LAETA-AEROG, Universidade da Beira Interior, Covilhã, Portugal
[2]ISEC Lisboa, Portugal
[3]LAETA-IDMEC, Instituto Superior Técnico, Universidade de Lisboa, Portugal

## Abstract

Earth's atmosphere is humanity's last defence against the potential threat of asteroid impacts. To assess the impact risk and devise effective mitigation strategies, it is essential to understand the interaction between asteroids and the atmosphere. This paper presents a comprehensive study that employs a system of differential-algebraic equations (DAEs) to model the trajectory and associated physical processes involved in an atmospheric entry and the consequent impact of an asteroid. The Apophis asteroid is utilized as a case study to compare and evaluate the performance of two numerical methods for solving these equations. The findings from this research contribute to advancing our understanding of asteroid entry dynamics and provide valuable insights for enhancing asteroid impact mitigation strategies. The Apophis asteroid, represented as a 340 m diameter sphere with a density of 3190 kg.m$^{-3}$, enters the atmosphere at a velocity of 30759 m.s$^{-1}$ and a 45-degree angle from an altitude of 81 km. The first method employed is the 4th-order Runge-Kutta method (RK4) with a constant time-step, commonly used for solving highly non-linear problems like this. The second method is based on the Dormand-Prince method, which utilizes a dynamic time step and provides a 4th-order solution with error estimation using a 5th-order solution. Computational efficiency and the resulting solutions are compared between the two methods. The study finds that the Dormand-Prince method offers a more accurate numerical solution with less computational effort. However, both approaches demonstrate a correspondence of at least three significant digits, confirming their validity. Overall, during its traversal through the atmosphere, the Apophis asteroid experiences a decrease in initial velocity by 0.83%, a loss of 22% of its initial mass, and a variation in its angle with the horizontal by 1.5%.

**Keywords:** Asteroid, Apophis, Dormand Prince, Runge Kutta

## 1. Introduction

Asteroids colliding with Earth pose an existential threat to civilisations. While the Earth's atmosphere acts as a barrier against cosmic objects, events releasing energy comparable to the Hiroshima nuclear bomb occur annually at high altitudes, avoiding ground impact [1]. While the probability of an individual experiencing an asteroid impact is low, the potential consequences are significant, making it difficult for people focused on day-to-day concerns to comprehend. The impact hazard shares similarities with destructive natural processes like earthquakes, fires, and floods, but with the potential for simultaneous devastation [2]. Studies on asteroid impacts reveal insights into their consequences. Collins et al. [3] quantified impact processes and their effects, showing seismic shaking as the most widespread, followed by ejecta deposition and air-blast pressure, with thermal radiation being highly destructive near impact sites. Svetsov [4] found that significant collisions can vaporize water layers and create uninhabitable rock vapour atmospheres. Wünnemann et al. [5] discovered that preventing cratering in the ocean floor requires a water depth 6-8 times the asteroid's diameter, with distinct rim and collapse waves generated by water impacts. Rumpf et al. [6] developed vulnerability models, highlighting aero-thermal effects as major contributors to surface impact losses, while offshore impacts exhibit decreasing vulnerability. Morais et al. [7] assessed the consequences of a hypothetical

Apophis asteroid impact on the ocean, determining that deep-ocean collisions result in inconsequential crater formation, seismic shaking, and material ejection, with tsunamis posing the greatest threat. Morais et al. [8] further analysed regional consequences, estimating casualties for Portuguese municipalities and emphasizing the importance of understanding and preparing for potential asteroid impacts.

This comparative study focuses on the asteroid Apophis, estimated to have a diameter of 340 meters [9]. Apophis is an Sq-class asteroid resembling low iron, low metal (LL) ordinary chondrite meteorites [10], with an average bulk density of 3.19 g.cm$^3$ [11]. Initially, Apophis gained attention due to its non-trivial impact probability with Earth in 2029, but updated observations dismissed this scenario [12, 13, 14]. However, there is a possibility of a collision in 2036 [15], which later diminished, resulting in a Torino Scale rating of 0 [16, 17]. Although Apophis will make a close approach in 2068, this possibility has been ruled out as of 2021, and it is no longer on NASA's Sentry Risk Table [18, 19].

Before an asteroid impact occurs, it must pass through the Earth's atmosphere. Understanding the effect of atmospheric passage on the asteroid's trajectory and physical properties is crucial for establishing a relationship between pre-entry and pre-impact characteristics. Meteor physics theory enables the description of a space body's ballistics through Earth's surface using a system of differential equations [20] solvable through numerical methods.

## 2. Modelling

### 2.1 Physical Model

The physical model utilizes the International Standard Atmosphere (ISA) model to determine air properties up to an altitude of 81 km. A two-dimensional X-Y coordinate system is adopted as the reference frame, with its origin located at the center of the Earth and co-rotating with the Earth, Figure 1.

The physical model assumes the Earth as a circle with radius $R_e$ and the atmosphere as an annulus with a thickness of $h_{max}$ The asteroid, with radius $R_a$ and density $\rho_a$, pierces the atmosphere at an angle $\alpha$ with the horizontal. Figure 2 depicts the variables that characterise the asteroid's position along the trajectory. These variables include the asteroid's position $\vec{r}$, which gives the asteroid altitude, and the velocity $\vec{v}$, whose initial direction is determined by the entry angle $\alpha$ and mainly governs the asteroid's trajectory. The altitude of the asteroid $h$ is the difference between the position vector magnitude and Earth's radius. The angle $\theta$ is the angle between the velocity and position vectors. When $h = 0$, $\theta$ represents the impact angle. Two main aspects of meteor physics describe the ballistics of a space body passage through Earth's surface: the dynamic aspect, *i.e.* the description of the asteroid's motion in the atmosphere, and the physical aspect, *i.e.* the interaction of the asteroid with the oncoming airflow [20]. Consequently, the simple physical theory focuses on the deceleration and mass loss of a non-fragmented body in the atmosphere, assuming constant drag $c_d$ and heat transfer $c_h$ coefficients. The first fundamental equation represents the momentum of the asteroid under applied forces, such as gravity and aerodynamic drag, with the assumption that the momentum lost by the asteroid is proportional to the momentum of the oncoming airflow.

$$m\frac{d\vec{v}}{dt} = -\frac{1}{2}c_d\rho_h v^2 S\frac{\vec{v}}{v} - m\frac{Gm_e}{r^3}\vec{r} \tag{1}$$

In equation (1), $m$ is the asteroid's mass, $t$ is time, $\rho_h$ is the air density at altitude $h$, $v$ is the magnitude of the asteroid's velocity vector, $S$ is the body's middle cross-section area, $G$ is the gravitation constant, $m_e$ is Earth's mass, and $r$ is the magnitude of the radius vector. The contribution of the lifting force in equation (1) is not present, as the asteroid is assumed spherical. The Coriolis and centrifugal forces in the rotating reference frame, along with the stratospheric winds, are negligible compared to the hypersonic velocity of the asteroid. The drag coefficient $c_d$ expresses the portion of the flow's momentum that decelerates the body. According to multiple authors [21, 22, 23], $c_d = 0.9$ is a reasonable assumption for a hypersonic sphere in the atmosphere. In addition, we can define $\vec{v}$ as the derivative of the radius as a function of time:

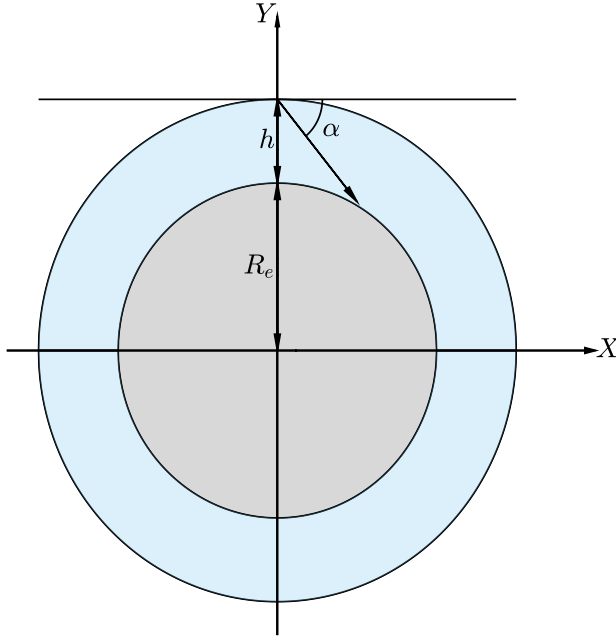$$\frac{d\vec{r}}{dt} = \vec{v} \tag{2}$$

Figure 1 – Coordinate system $X - Y$ of the atmospheric traverse of an asteroid. The thickness of the atmosphere is exaggerated for representation purposes.
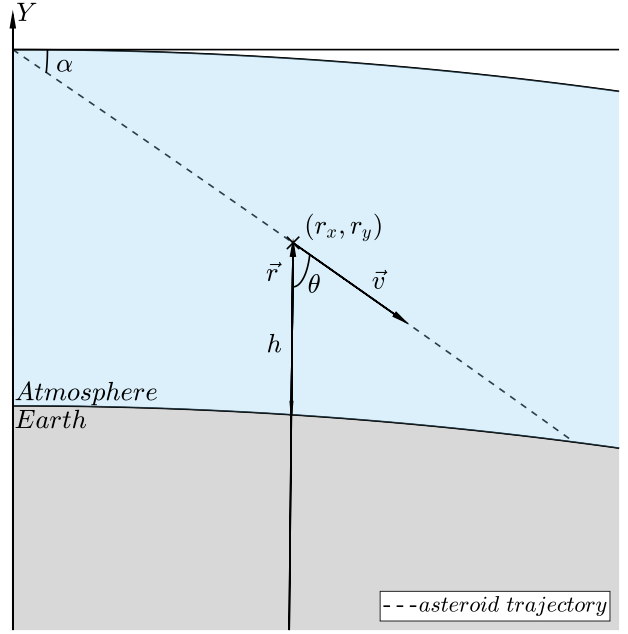
Figure 2 – Schematic representation of a potential asteroid's trajectory and its defining parameters.

The area $S$ is obtained as a function of the current asteroid mass $m$, its initial mass $m_0$, and initial cross-sectional area $S_0$:

$$S = S_0 \left( \frac{m}{m_0} \right)^{\mu} \tag{3}$$

Assuming the material loss from the asteroid's surface is isotropic, *i.e.* the object does not deform and remains a sphere, the parameter of shape variation $\mu$ corresponds to $2/3$ as defined by Bronshten [20].

The second fundamental relation in meteor physics is the mass-loss equation that assumes that a ratio $c_h$ of the kinetic energy of the oncoming stream of molecules is expended on the ablation of the asteroid. Assuming $H$ is the specific heat of sublimation of the asteroid's material, the equation takes the form:

$$\frac{dm}{dt} = -\frac{c_h \rho_h v^3 S}{2H} \tag{4}$$

The heat transfer coefficient $c_h$ depends on the asteroid's velocity, the flight altitude, the air density, the boundary layer temperature, the dissociation and ionization processes in the boundary layer, and the absorption coefficient, among others. In the literature, the commonly accepted value is $c_h = 0.1$ [20, 22, 24].

## 2.2 Numerical Model

The 4th order Runge-Kutta (RK4) method is commonly used for solving simultaneous non-linear equations [22, 25, 26]. It approximates the solution at discrete time steps by evaluating the derivative of the function at multiple points within each step. The method estimates the slope of the solution curve using a weighted average of these derivatives, providing a more accurate prediction of the next point. To determine the stopping criterion for an asteroid's impact on the surface, the altitude reaching zero is considered. Discretization errors are estimated by performing three simulations with progressively finer grids.

The Dormand-Prince (RKDP) method is a widely used numerical algorithm that efficiently approximates the solution of ordinary differential equations with adaptive step size control. It uses a fourth-fifth order Runge-Kutta approach to calculate intermediate approximations. By comparing the fourth-

and fifth-order approximations, the method estimates the local truncation error and adjusts the step size accordingly, maintaining accuracy within predefined tolerances. The RKDP method selects an appropriate number of steps with dynamic intervals, adjusting the time step based on a pre-established tolerance. For the Apophis case study, a tolerance value of $10^9$ is used. This adaptive step size control enables the method to dynamically adapt and balance accuracy with computational efficiency

## 3. Results and Discussion

To simulate the Apophis atmospheric passage, the initial conditions of the asteroid must be established, including its diameter $D_a$, velocity $v_a$, density $\rho_a$, and entry angle $\alpha$. Table 1 presents the assumed values of Apophis' initial properties.

Table 1 – Apophis initial physical properties [9, 10]

| $D_a$ [m] | $v_a$ [m/s] | $\rho_a$ [kg.m$^{-3}$] | $\alpha$ [deg] |
|---|---|---|---|
| 340 | 30756 | 3190 | 45 |

The diameter and density of Apophis are well-established in the literature. However, its entry velocity depends on the position along its orbit at the time of its close approach with Earth. As Apophis is no longer a threat to Earth, the periods of closest approach that could result in an impact are no longer relevant. Therefore, the magnitude of Apophis entry velocity is assumed to be the mean orbital speed of Apophis [27].

The initial conditions for solving the differential-algebraic system of equations (DAE) can be determined by setting the entry point at position $X = 0$, where the $Y$ coordinate represents the full distance between Apophis and the center of the Earth. These initial conditions, as shown in Table 2, depend on the given physical parameters. The initial velocities $v_{x,0}$ and $v_{y,0}$ are the projections of the velocity vector in the respective $X$ and $Y$ axis. The initial mass of Apophis assumes the asteroid is an homogeneous sphere of density $\rho_a$, resulting in a circular cross sectional area $S_0$. The initial density $\rho_0$ is the air density at the entry altitude $h_{max}$. By setting $t_0 = 0$, the numerical method can be initiated once the integration step $s$ is established. To choose the initial step, a time scale was computed based on the asteroid's properties:

$$s = \frac{D_a}{4v_a} \tag{5}$$

To obtain units of time, the Apophis radius $D_a/2$ was divided by its entry velocity $v_a$. To further ensure the time independence, this result was divided in half. To validate the results, and to ensure independence from the chosen time step, three consecutive simulations were performed with increasingly smaller steps, Table 3.

Table 2 – Definition of the Apophis' atmospheric entry initial conditions

| $r_{x,0}$ [m] | $r_{y,0}$ [m] | $v_{x,0}$ [m.s$^{-1}$] | $v_{y,0}$ [m.s$^{-1}$] | $m_0$ [kg] | $S_0$ [m$^2$] | $\rho_0$ [kg.m$^{-3}$] |
|---|---|---|---|---|---|---|
| 0 | $R_e + h_{max}$ | $v_a \cos(\alpha)$ | $-v_a \sin(\alpha)$ | $\rho_a \pi D_a^3/6$ | $\pi D_a^2/4$ | $p/RT$ |
| 0 | $6.452 \times 10^6$ | $2.175 \times 10^4$ | $-2.175 \times 10^4$ | $6.585 \times 10^{10}$ | $9.079 \times 10^4$ | $1.570 \times 10^{-5}$ |

Table 3 – Final properties of the atmosphere passage of Apophis in three different simulations

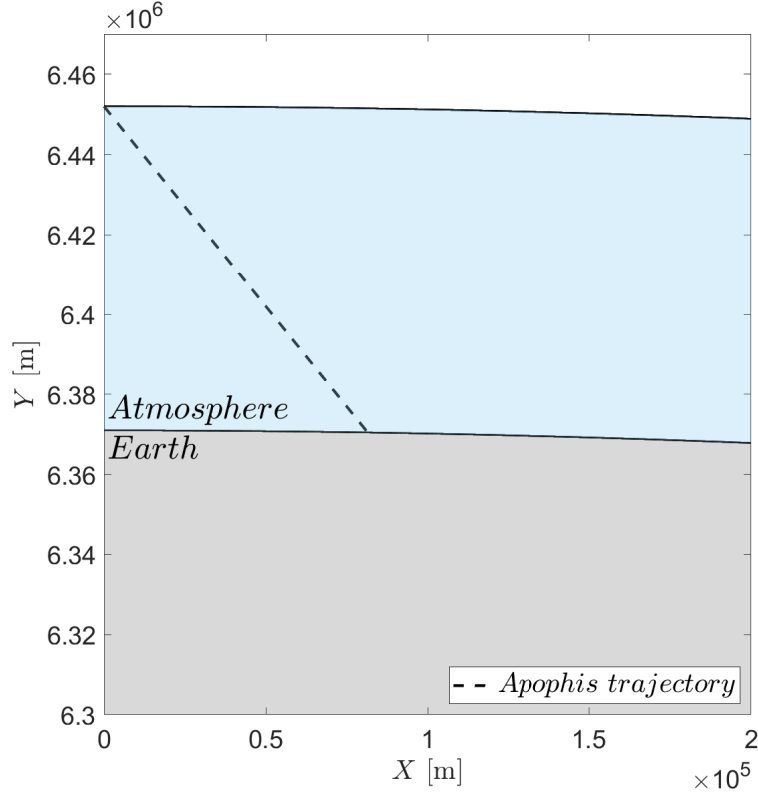| | $t_n$ [s] | $h_n$ [m] | $v_n$ [km.s$^{-1}$] | $m_n \times 10^{-8}$ [kg] | $\theta_n$[deg] |
|---|---|---|---|---|---|
| $s$ | 3.7503 | 40.445 | 30.4905 | 512.974 | 44.3158 |
| $s/2$ | 3.7503 | 11.145 | 30.4890 | 512.302 | 44.3156 |
| $s/4$ | 3.7496 | 11.212 | 30.4888 | 512.197 | 44.3156 |

Figure 3 – Apophis trajectory through Earth's atmosphere. The dashed line corresponds to the coordinate pair $(r_{x,i}, r_{y,i})$ over the entire time $t$ computed.

At first glance, the results seem to be converging with each additional simulation. Furthermore, observing the Figures 3 and 4, the solution seem stable as the three simulations overlap each other and are indistinguishable. In less than four seconds the asteroid travels from the entry point at $81$ km to the surface, this is mainly due to its high speed and entry angle. From observing Figure 3, Apophis trajectory seems a straight line and Earth's curvature is barely noticeable. The absence of a perceptible curvature is due to the low horizontal distance the Apophis traverses compared to Earth's radius. Apophis almost straight trajectory can also be explained, albeit through more elaborate means. In the employed model, two distinct forces dictate the direction of Apophis trajectory - the drag force and the gravitational force. Initially, the direction of the trajectory is defined by the entry velocity $\vec{v}$ and the respective entry angle, the drag force acts exactly in opposition, so it will only affect its magnitude and not the direction of the velocity, the gravitational force acts in the direction of Earth's center and its thereby the only force responsible for the change in direction. Due to the Apophis high initial velocity and short time on the atmosphere, gravity does not affect the direction in a major way. Figure 4 shows the variations of velocity and mass along the Apophis trajectory. Both velocity and mass depict a similar behaviour, having slight changes in the first two thirds of its trajectory, followed by a sudden drop in the last third. Furthermore, before significantly decreasing, the velocity slightly increases throughout the majority of the trajectory. This increase in velocity means that the force of gravity surpasses the drag force in magnitude due to the low air density at higher altitudes. As the altitude decreases and consequently the density increases, the drag force increases significantly, decreasing the velocity and the mass.

However, to properly validate the results and find the discretisation error, a grid convergence study is necessary. Even though the reference frame utilised has two spatial dimensions, the grid is one dimensional as it corresponds to the trajectory of the asteroid, meaning there is a dependency between the $X$ and $Y$ coordinates. Additionally, the time and space domains are also interconnected, because for a given time $t_i$ there is only one set of correspondent coordinates $(r_{x,i}, r_{y,i})$. The grid refinement ratio is $2$, because the step is reduced in half in each subsequent simulation. As the time step is
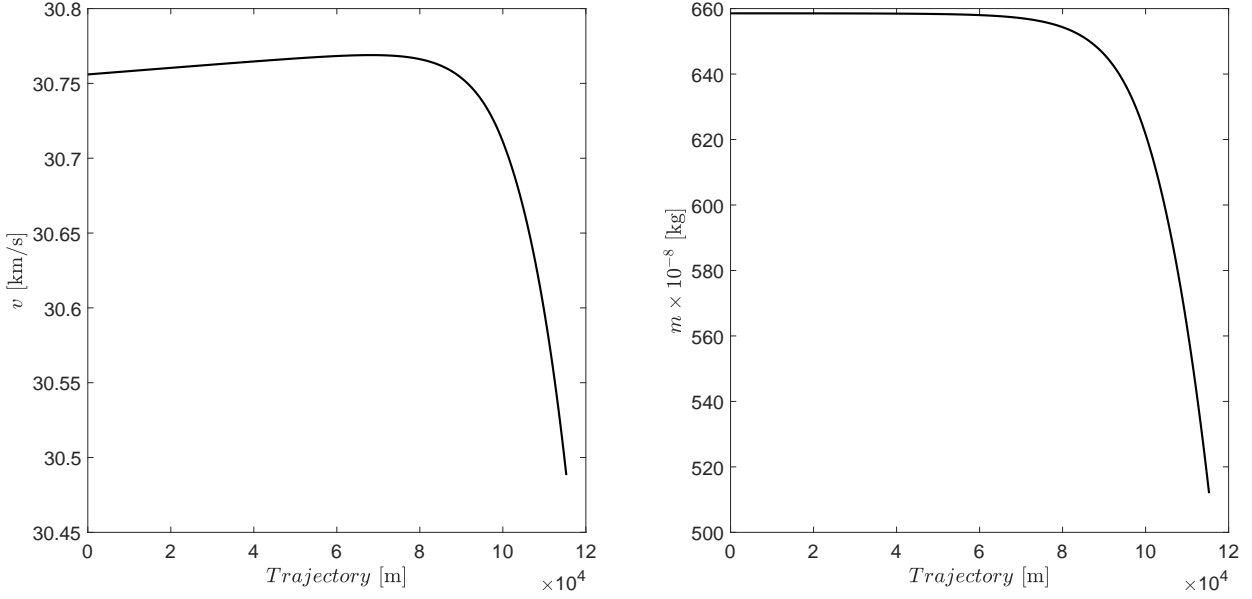
5

Figure 4 – Apophis velocity magnitude variation and mass-loss along its trajectory through Earth's atmosphere obtained via the 4th-order Runge-Kutta method.

refined, the discretisation error should asymptotically approach zero, excluding computer round-off errors. However, the mass and velocity values from Table 3 cannot be used in the convergence study because they correspond to different values of time. To properly validate the results, solutions computed for the same $t$ must be compared. Thus, Table 4 presents the mass and velocity solutions for $t = 3.7476$ s.

Table 4 – Grid convergence study of the atmosphere passage of Apophis

|  | Grid Spacing | $m \times 10^{-8}$ [kg] | $v$ [km.s$^{-1}$] | $c_m$ | $c_v$ |
|---|---|---|---|---|---|
| 0 | 0 | 512.555 | 30.4896 | | |
| $s/4$ | 1 | 512.892 | 30.4904 | $8.20387 \times 10^{-4}$ | $3.13506 \times 10^{-5}$ |
| $s/2$ | 2 | 513.227 | 30.4911 | $1.63665 \times 10^{-3}$ | $6.25181 \times 10^{-5}$ |
| $s$ | 4 | 513.896 | 30.4926 | | |

The fourth-order Runge-Kutta method exhibits a theoretical order of convergence of 4. The order of convergence represents the rate at which the numerical solution approaches the exact result with diminishing step sizes. A convergence order of 4 implies that the error in the numerical solution diminishes approximately in proportion to the fourth power of the step size. Consequently, a higher-order convergence is advantageous as it enables accurate results even with relatively larger step sizes, thereby enhancing computational efficiency. However, it is noteworthy that the actual order of convergence is 1.00 for both mass and velocity, attributable to non-linearities inherent in the equations. Despite this deviation from the expected 4, the solutions remain within the asymptotic range of convergence. While the convergence rate is slower than anticipated, the associated error bands are narrow, indicative of the solutions closely aligning with the exact value. It is pertinent to acknowledge that this set of results does not align with the position $h = 0$, Table 4. Given the observed convergence and decreasing error bands, the final solution is obtained with the intermediate grid and employing the finer grid to assess the relative error. Consequently, the ultimate solutions for velocity and mass during the Apophis atmospheric passage are $30.4890 \pm 0.0002$ km.s$^{-1}$ and $512.302 \pm 0.105 \times 10^8$ kg, respectively. Throughout the atmospheric traverse, Apophis experiences a $0.868 \pm 0.001\%$ reduction in velocity and a $22.2 \pm 0.016\%$ decrease in mass.

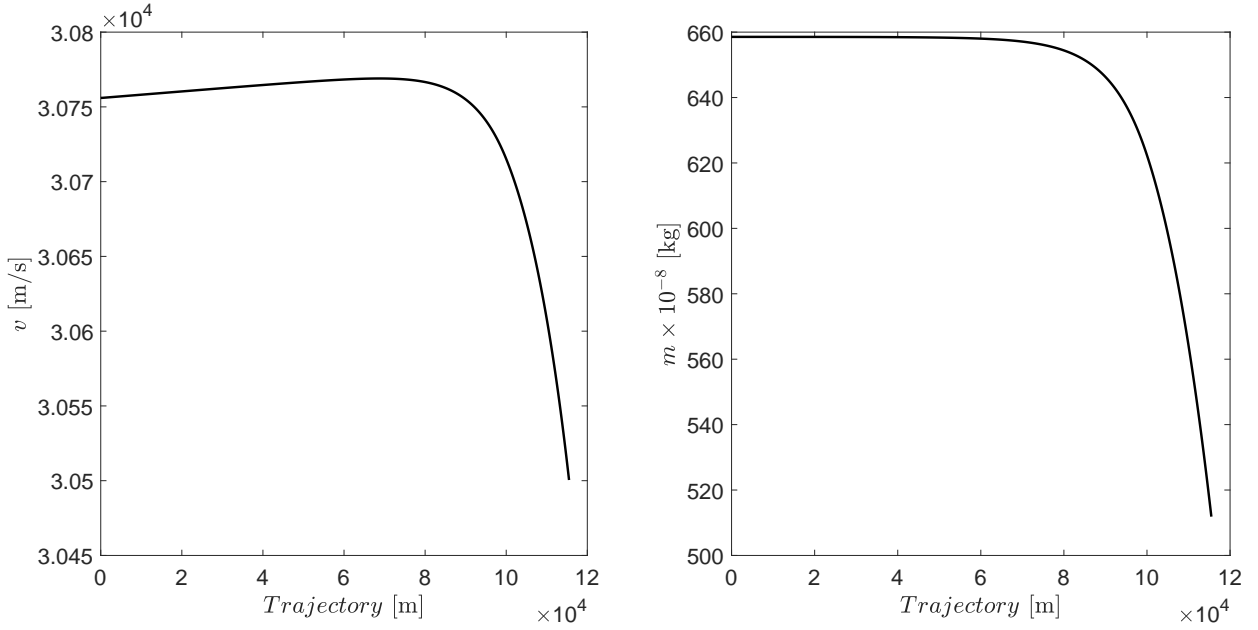Despite not knowing the error between the results and the true physical solution of the equations,

Figure 5 – Apophis velocity magnitude variation and mass-loss along its trajectory through Earth's atmosphere obtained through the RKDP.

Apophis diameter estimate is $340 \pm 40$ m, meaning its total mass, assuming an homogeneous sphere of density $\rho_a = 3190$ kg.m$^{-3}$, ranges from $4.52 \times 10^{10}$ kg to $9.19 \times 10^{10}$ kg. The mass uncertainty range is three orders of magnitude larger than the estimated final mass error.

Figure 5 depicts the variation of velocity and mass along the Apophis trajectory obtained with the RKDP method. The final solution converged until $t_n = 3.7493$, where the altitude was $h_n = 6.2 \times 10^{-4}$. At this point, the velocity and mass of Apophis atmosphere traverse are $v_n = 30.5004$ km.s$^{-1}$ and $m_n = 511.861 \times 10^8$ kg, respectively. With this trajectory, the impact angle of Apophis is $\theta_n = 44.3155$ deg. Due to the traverse of Apophis through Earth's atmosphere, the asteroid loses $0.83\%$ of its initial velocity and $22\%$ of its initial mass. Table 5 compares the solution of both numerical methods.

Table 5 – Comparison of the final results of the Apophis passage through Earth's atmosphere obtain with different numerical methods

|  | $t_n$ [s] | $h_n$ [m] | $v_n$ [km.s$^{-1}$] | $m_n \times 10^{-8}$ [kg] | $\theta_n$[deg] |
|---|---|---|---|---|---|
| RK4 | 3.7503 | 11.145 | $30.4890 \pm 0.0002$ | $512.302 \pm 0.105$ | 44.3156 |
| RKDP | 3.7493 | 00.00062 | 30.5004 | 511.861 | 44.3155 |

## 4. Conclusions

This study focused on the outcome of the Apophis atmospheric passage obtained through two numerical methods. The final altitude reached by Apophis is the most notable outcome, clearly showing a significant difference between the two methods employed. The RKDP method resulted in an altitude of five orders of magnitude closer to zero than the estimate obtained using the RK4 constant-step method. Moreover, the dynamic-step model required much less computational effort than the constant-step method. The results obtained from both methods exhibit a correspondence of at least three significant digits, reinforcing the methods' validity and implementation. However, it is fundamental to note that although the numerical solution obtained through the system of equations was successful, there may still be a difference between the numerical and physical solutions. Additionally, the physical methods used in the study have limitations, which can affect the accuracy of the solution. Therefore, using more complex and realistic physical models can yield better and more accurate results, as the ultimate goal of physical modelling is to emulate real-world conditions and limitations.

## 5. Contact Author Email Address

renatohenriques2@hotmail.com
luis.santos@iseclisboa.pt
andre@ubi.pt
ruimelicio@gmail.com

## 6. Copyright Statement

## 7. Acknowledgements

## References

[1] Clark R. Chapman and David Morrison. Impacts on the Earth by asteroids and comets: Assessing the hazard. *Nature*, 367(6458):33–40, 1994.

[2] Clark R. Chapman. The hazard of near-Earth asteroid impacts on earth. *Earth and Planetary Science Letters*, 222(1):1–15, 2004.

[3] Gareth S. Collins, H. Jay Melosh, and Robert A. Marcus. Earth Impact Effects Program: A Web-based computer program for calculating the regional environmental consequences of a meteoroid impact on Earth. *Meteoritics and Planetary Science*, 40(6):817–840, 2005.

[4] Vladimir V. Svetsov. Numerical simulations of very large impacts on the Earth. *Planetary and Space Science*, 53(12):1205–1220, 2005.

[5] K. Wünnemann, G. S. Collins, and R. Weiss. Impact of a cosmic body into Earth's Ocean and the generation of large tsunami waves: Insight from numerical modeling. *Reviews of Geophysics*, 48(4):1–26, 2010.

[6] Clemens M. Rumpf, Hugh G. Lewis, and Peter M. Atkinson. Population vulnerability models for asteroid impact risk assessment. *Meteoritics and Planetary Science*, 52(6):1082–1102, 2017.

[7] Renato H. Morais, Luís F. F. M. Santos, André R. R. Silva, and Rui Melicio. Hypothetical Apophis deep ocean impactEnergy analysis. *Acta Astronautica*, 188(November):438–450, 2021.

[8] Renato H. Morais, Luís F. F. M. Santos, André R. R. Silva, and Rui Melicio. Short-Term Consequences of Asteroid Impacts into the Ocean : A Portuguese Case Study. *Universe*, 8(5):1–27, 2022.

[9] Akash Satpathy, Amy Mainzer, Joseph R. Masiero, Tyler Linder, Roc M. Cutri, Edward L. Wright, Jana Pittichová, Tommy Grav, and Emily Kramer. NEOWISE Observations of the Potentially Hazardous Asteroid (99942) Apophis. *The Planetary Science Journal*, 3(5):124, 2022.

[10] Richard P. Binzel, Andrew S. Rivkin, Cristina A. Thomas, Pierre Vernazza, Thomas H. Burbine, Francesca E. DeMeo, Schelte J. Bus, Alan T. Tokunaga, and Mirel Birlan. Spectral properties and composition of potentially hazardous Asteroid (99942) Apophis. *Icarus*, 200(2):480–485, 2009.

[11] D. T. Britt, D. Yeomans, K. Housen, and G. Consolmagno. Asteroids Density, Porosity, and Structure. In W. Bottke, A. Cellino, P. Paolicchi, and R. P. Binzel, editors, *Asteroids III*, chapter 4.2, pages 485–500. University of Arizona Press, Tucson, AZ, USA, 2002.

[12] Steven R. Chesley. Potential impact detection for near-Earth asteroids: The case of 99942 Apophis (2004 MN4). *Proceedings of the International Astronomical Union*, 1(S229):215–228, 2005.

[13] Jon D. Giorgini, Lance A.M. Benner, Steven J. Ostro, Michael C. Nolan, and Michael W. Busch. Predicting the Earth encounters of (99942) Apophis. *Icarus*, 193(1):1–19, 2008.

[14] Marina Brozović, Lance A.M. Benner, Joseph G. McMichael, Jon D. Giorgini, Petr Pravec, Petr Scheirich, Christopher Magri, Michael W. Busch, Joseph S. Jao, Clement G. Lee, Lawrence G. Snedeker, Marc A.

Silva, Martin A. Slade, Boris Semenov, Michael C. Nolan, Patrick A. Taylor, Ellen S. Howell, and Kenneth J. Lawrence. Goldstone and Arecibo radar observations of (99942) Apophis in 20122013. *Icarus*, 300:115–128, jan 2018.

[15] D. Farnocchia, S. R. Chesley, P. W. Chodas, M. Micheli, D. J. Tholen, A. Milani, G. T. Elliott, and F. Bernardi. Yarkovsky-driven impact risk analysis for asteroid (99942) Apophis. *Icarus*, 224(1):192–200, 2013.

[16] David Vokrouhlický, Davide Farnocchia, David Čapek, Steven R. Chesley, Petr Pravec, Petr Scheirich, and Thomas G. Müller. The Yarkovsky effect for 99942 Apophis. *Icarus*, 252:277–283, 2015.

[17] Peng Guo, V. V. Ivashkin, C. A. Stikhno, and P. M. Shkapov. Determination and investigation of asteroid Apophis' trajectories set potentially colliding with the Earth in 2036. *IOP Conference Series: Materials Science and Engineering*, 468(1), 2018.

[18] I. Wlodarczyk. The potentially dangerous asteroid (99942) Apophis. *Monthly Notices of the Royal Astronomical Society*, 434(4):3055–3060, 2013.

[19] Jorge A. Pérez-Hernández and Luis Benet. Non-zero Yarkovsky acceleration for near-Earth asteroid (99942) Apophis. *Communications Earth & Environment*, 3(1):1–5, 2022.

[20] V. A. Bronshten. *Physics of Meteoric Phenomena*. D. Reidel Publishing Company, 1983.

[21] Leonid I. Turchak and Maria I. Gritsevich. Meteoroids interaction with the earth atmosphere. *Journal of Theoretical and Applied Mechanics (Poland)*, 44(4):15–28, 2014.

[22] Daniil E. Khrennikov, Andrei K. Titov, Alexander E. Ershov, Vladimir I. Pariev, and Sergei V. Karpov. On the possibility of through passage of asteroid bodies across the Earth's atmosphere. *Monthly Notices of the Royal Astronomical Society*, 493(1):1344–1351, 2020.

[23] Eric Loth, John Tyler Daspit, Michael Jeong, Takayuki Nagata, and Taku Nonomura. Supersonic and hypersonic drag coefficients for a sphere. *AIAA Journal*, 59(8):3261–3274, 2021.

[24] Barrett Baldwin and Yvonne Sheaffer. Ablation and breakup of large meteoroids during atmospheric entry. *Journal of Geophysical Research*, 76(19):4653–4668, 1971.

[25] L. R. Bellot Rubio, M. J. Martínez González, L. Ruiz Herrera, J. Licandro, D. Martínez Delgado, P. Rodríguez Gil, and M. Serra-Ricart. Modeling the photometric and dynamical behavior of Super-Schmidt meteors in the Earth's atmosphere. *Astronomy and Astrophysics*, 359:680–691, 2002.

[26] Davide Farnocchia, Peter Jenniskens, Darrel K. Robertson, Steven R. Chesley, Linda Dimare, and Paul W. Chodas. The impact trajectory of asteroid 2008 TC3. *Icarus*, 294:218–226, 2017.

[27] Jet Propulsion Laboratory. JPL Small-Body Database Browser: (Apophis). [Online]. Available: `https://ssd.jpl.nasa.gov/tools/sbdb_lookup.html#/?sstr=apophis`. [Accessed: 15-Mar-2023].